ACS Catalysis

Research Article

pubs.acs.org/acscatalysis

Tuning the Chemoselectivity of Rh Nanoparticle Catalysts by Site-Selective Poisoning with Phosphine Ligands: The Hydrogenation of Functionalized Aromatic Compounds

Dennis J. M. Snelders, Ning Yan, Weijia Gan, Gabor Laurenczy, and Paul J. Dyson*

Institut des Sciences et Ingénierie Chimiques, Ecole Polytechnique Fédérale de Lausanne (EPFL), CH-1015 Lausanne, Switzerland

Supporting Information

ABSTRACT: The hydrogenation of phenylacetone to cyclohexylacetone, in which the aromatic ring is selectively reduced in preference to the carbonyl group, has been achieved with chemoselectivities exceeding 90%. The catalyst (precatalyst) used to achieve this transformation comprises PVP-stabilized Rh nanoparticles dispersed in water with some phosphine ligand additives. Phosphine ligands with different steric and electronic properties and polarities were investigated for this purpose, and several clear trends were observed, showing the potential of well-defined phosphine ligands as modifiers in nanocatalysis.

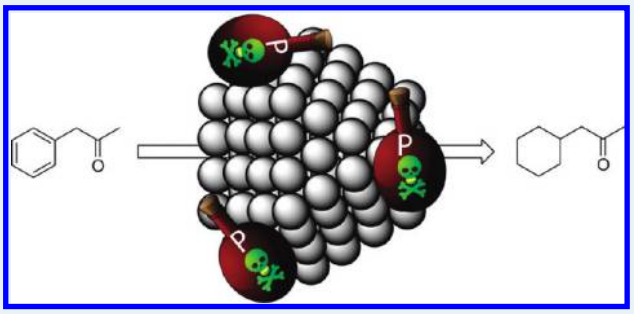

KEYWORDS: *nanoparticles, nanocatalysis, hydrogenation, selectivity, phosphine ligands, poisoning*

1. INTRODUCTION

The catalytic hydrogenation of aromatic substrates by soluble metal nanoparticle catalysts has recently attracted much interest due to their high activity and stability.[1−3] The use of water and other "green" solvents has become increasingly important in this field not only because of the possibility of facile product extraction but also because these solvents can influence the selectivity of the reaction.[4] Indeed, the chemoselective hydrogenation of aromatic rings in substrates that contain an aromatic group as well as other reducible functionalities is extremely challenging.[3] A few cases of chemoselective catalytic arene hydrogenation using a variety of heterogeneous catalysts[5,6] and metal nanoparticle catalysts[7−10] have been reported. Notably, polyvinylpyrrolidone (PVP)-protected Rh nanoparticles are known to be highly active hydrogenation catalysts for a range of substrates including arenes.[11−14] PVP is widely used to stabilize soluble metal nanoparticles,[15−17] and well-defined water-soluble PVP-stabilized Rh nanoparticles can be prepared in a simple, reproducible manner via the alcoholic reduction of $RhCl_3$.[18]

In addition to polymer stabilizers such as PVP, a variety of classical ligands that are used in coordination and organometallic chemistry, such as thiols, amines, and phosphines, may be used as stabilizers for metal nanoparticles, and such ligands may influence the formation of the nanoparticles.[3,16,19,20] In heterogeneous catalysis, ligands tend to be used as additives or poisons to modify the properties of the catalyst, such as chemoselectivity in hydrogenation reactions.[12,21−23] Poisoning by S-, P-, C-, and O-donor ligands has been used to determine the number of active sites on nanopartcle catalysts.[24−26] Triphenylphosphine has also been used as a modifier for Pd-cluster hydrogenation catalysts.[27] Schmid et al. described a series of supported palladium clusters that were stabilized by various N-based ligands, and the chemoselectivity in hydrogenation reactions of various substrates, including acetophenone, was dependent on the ligand employed.[28] Herein, we present a systematic study on the effects that sulfonated, water-soluble phosphine ligands have on the chemoselectivity of PVP-stabilized Rh nanoparticles in aqueous phase hydrogenation reactions. To the best of our knowledge, the approach used herein has not been explored before. Specifically, we show that selective site blocking on soluble nanoparticles can lead to significant improvements in chemoselectivity in challenging reactions.

2. RESULTS

2.1. Characterization of Phosphine Ligands. In this study, a series of sulfonated, water-soluble phosphine ligands (Figure 1) were used. In comparison with tppts (**1**), either one or two aryl substituents have been replaced with either a less sterically demanding methyl group or a more sterically demanding cyclopentyl group. Consequently, this set of phosphines can be assumed to have the following order of increasing steric demand: **2** < **3** < **1** < **5** < **4**. To evaluate the electronic properties of these phosphine ligands, the corresponding phosphine selenides were synthesized by reaction with elemental selenium, and the coupling constants $^1J_{P,Se}$ in the ^{31}P NMR spectra of the phosphine selenides were measured. This coupling constant is roughly inversely proportional to the phosphine basicity; that is, more basic phosphines

Received: November 6, 2011
Revised: December 21, 2011
Published: December 21, 2011

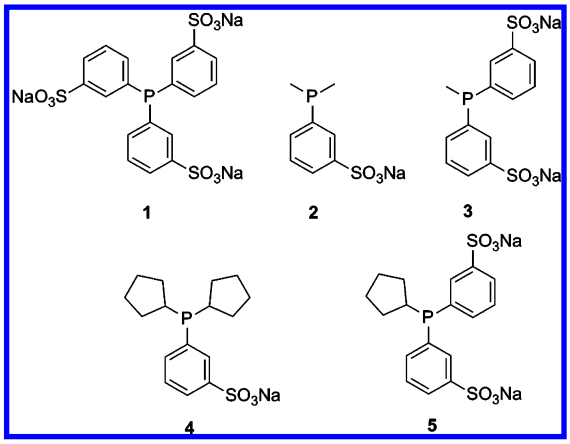

Figure 1. Sulfonated phosphine ligands **1**–**5**.

lead to smaller $^{1}J_{P,Se}$ coupling constants.[29−31] Table 1 shows the data that were observed for each of the phosphine selenides

Table 1. $^{1}J_{P,Se}$ Coupling Constants Observed in the ^{31}P-NMR Spectra of L(Se) (L = 1−5)

	$^{1}J_{P,Se}$ of L(Se)(Hz)	
ligand	CD_3OD	D_2O
1	756	707
5	742	685
3	733	677
4	716	660
2	702	642

L(Se) (L = **1**−**5**). Measurements were performed in both CD_3OD and D_2O, and in both solvents, the same trend was observed, showing the following order of increasing phosphine basicity: **1** < **5** < **3** < **4** < **2**.

2.2. Preparation and Characterization of Phosphine-Modified, PVP-Stabilized Rh Nanoparticles. PVP-stabilized Rh nanoparticles were synthesized by alcoholic reduction of $RhCl_3$ in the presence of PVP (ratio PVP/Rh = 20). Subsequently, the phosphine ligands were added (ratio phosphine/Rh = 0.5). To investigate the possible effect of the added phosphine ligands on the morphology of the nanoparticles, TEM analysis was carried out for samples containing PVP-stabilized Rh nanoparticles in the presence of phosphine ligands **1**, **2**, and **4** and as a control on a phosphine-free sample. The stability of the NPs under catalytic conditions was also evaluated for the hydrogenation of cyclohexanone under biphasic conditions as a model reaction. Figure 2 shows the TEM images and nanoparticle size distributions obtained for the control sample and for the sample containing ligand **4**, both before and after catalysis. The TEM images and size distributions for the samples containing **1** and **2** are provided in the Supporting Information. The TEM images show that in the absence of a phosphine ligand, nanoparticles with a diameter of about 3−4 nm are obtained and that after catalysis, considerable agglomeration of the nanoparticles has taken place, but no significant change in the size of the individual nanoparticles was observed. This agglomeration process is in accordance with previous observations.[14] Importantly, the addition of phosphine ligands **1**, **2**, or **4** had no significant effect on the nanoparticle size distributions.

To further characterize the nanoparticle surface, IR spectra were recorded after exposure of the PVP-Rh and PVP-Rh/phosphine mixtures to a CO atmosphere; see the Supporting Information for the spectra. In the absence of the phosphine and after CO exposure for 2 h, the obtained IR spectrum featured three bands at 2073, 2027, and 1997 cm^{-1}. In the presence of phosphine, the IR spectrum changes dramatically with each phosphine, giving rise to a distinct spectrum. For phosphines **1**, **3**, **4**, and **5**, a similar behavior was observed, where the band at 2073 cm^{-1} disappears, the band at 2027 cm^{-1} remains nearly unchanged, and the band at 1997 moves to lower wavenumber; that is, 1983 cm^{-1} for **1**, 1976 cm^{-1} for **3**, 1962 cm^{-1} for **4**, and 1968 cm^{-1} for **5**. For **2**, the peaks at 2073 and 1997 cm^{-1} became much more intense.

2.3. Catalytic Hydrogenations. *2.3.1. Hydrogenation of Model Substrates.* The hydrogenation activity of the water-soluble, PVP-stabilized Rh nanoparticles in the presence of phosphine ligands **1**−**5** was studied for three different model substrates: cyclohexanone, toluene, and phenol (Scheme 1). In the case of cyclohexanone and toluene, catalysis was performed under biphasic, aqueous−organic conditions, whereas for phenol, a single phase was formed. Note, all the phosphine ligands are soluble in the aqueous phase.

In the absence of phosphine ligands, at room temperature and at a H_2 pressure of 10 bar, high conversion was observed for all three substrates in 5 h. In general, the addition of phosphine ligands at a phosphine-to-Rh molar ratio of 0.5 led to a decrease in the catalytic activity, but the extent of this decrease varies with the phosphine ligand and the substrate employed. For cyclohexanone, ligands **2**, **3**, and in particular, **4** significantly inhibited the catalytic activity (Figure 3). In contrast, the presence of **1** or **5** hardly affected the activity. High conversions were observed at a substrate-to-rhodium ratio of 375. Increasing this ratio to 770 reduced the conversions, allowing clearer trends between the different ligands to be appreciated.

Two different aromatic substrates, toluene and phenol, were selected to evaluate the activity of the system for arene hydrogenation (Figure 4). For both substrates, ligands **1** and **5** hardly affected the activity, and ligand **3** slightly inhibited the activity. Ligand **2**, however, significantly inhibited the hydrogenation of both substrates, especially toluene, and notably, ligand **4** suppressed the hydrogenation of phenol but not of toluene.

2.3.2. Chemoselective Hydrogenation of Phenylacetone. As a result of the presence of phosphine ligands, a pronounced difference is observed for the activity of the nanoparticles for the hydrogenation of the three different model substrates, with **2** and **4** inhibiting the hydrogenation of the C═O bond most effectively. Moreover, **4** only slightly impedes the hydrogenation of the aromatic ring in toluene. These differences led us to explore the possibility of using these systems for the chemoselective hydrogenation of phenylacetone, that is, a substrate containing both an aromatic ring and a carbonyl group (Scheme 2). Hydrogenation yields a mixture of 1-phenyl-2-propanol (**6**, as a result of hydrogenation of the carbonyl group), cyclohexylacetone (**7**, as a result of arene hydrogenation), and the fully hydrogenated product 1-cyclohexyl-2-propanol (**8**).

Phenylacetone proved to be less reactive than the model substrates mentioned above, necessitating more forcing reaction conditions (50−80 °C, 30 bar H_2). In the absence of the phosphine ligands, the dominant product is **7** (~70%).

dx.doi.org/10.1021/cs200575r | ACS Catal. 2012, 2, 201−207

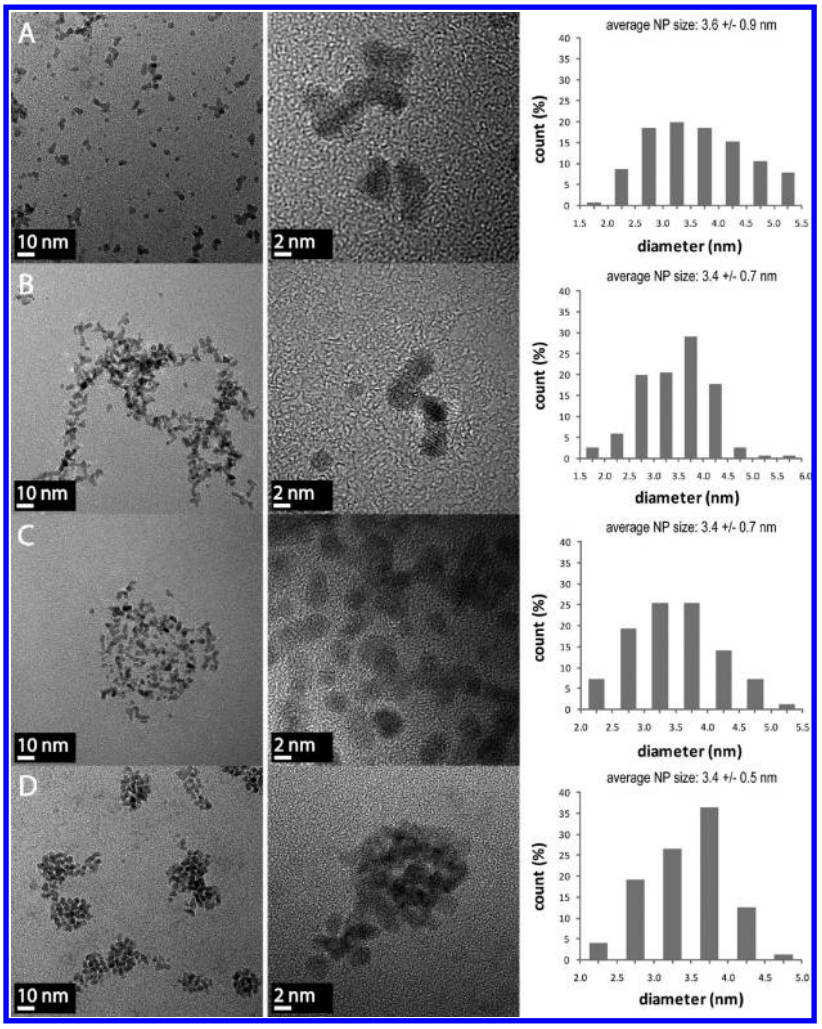

Figure 2. TEM (left) and HRTEM (center) images and size distributions (right) of PVP-stabilized Rh NPs. A: in the absence of a phosphine ligand, before catalysis. B: in the absence of a phosphine ligand, after catalysis. C: in the presence of phosphine ligand **4** (**4**/Rh = 0.5), before catalysis. D: in the presence of phosphine ligand **4** (**4**/Rh = 0.5), after catalysis.

Scheme 1. Catalytic Hydrogenation of Cyclohexanone, Toluene or Phenol by PVP-Stabilized Rh Nanoparticles in the Presence of Phosphine Ligands

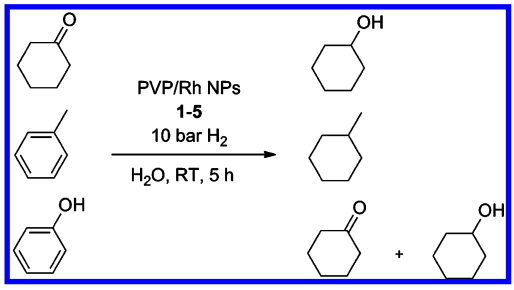

All three phosphine ligands led to a slight increase in the chemoselectivity for **7** (Figure 5). As expected from the hydrogenation of the model substrates, the largest increase in selectivity toward **7** was observed with PVP-Rh/**4**, giving a selectivity of 84%, albeit with a decrease in the conversion.

To further improve the catalytic performance of the nanoparticles toward higher chemoselectivity, the reaction conditions were optimized in the presence of **4** (Table 2). It was found that changing the phosphine-to-rhodium ratio strongly influenced both the conversion and the selectivity. A decrease in this ratio led to a higher conversion, and the selectivity for **7** reached 90% with a conversion of 80% at a ratio of 0.1. A further slight increase of the selectivity could be achieved by reducing the temperature, but with a reduction in the conversion. Changing the PVP-to-rhodium ratio from 20 to 10 did not significantly affect the performance of the system. The influence of the solvent was also investigated, and it was found that performing the reaction in MeOH under the same conditions gave full conversion, but with a lower selectivity.

3. DISCUSSION

Herein, we observed that the catalytic performance of PVP-stabilized Rh nanoparticles in water can be significantly modified by the addition of hydrophilic phosphines, **1**−**5**. TEM analysis of the nanoparticles did not show a significant influence of the phosphine ligands on the morphology of the nanoparticles, indicating that the differences in catalytic performance can be attributed to the modification of the nanoparticle surface (site blocking) due to coordination of the phosphine ligands. The IR spectra of the phosphine-modified nanoparticles after CO exposure differed for each of the phosphines, indicating that each of the different phosphine ligands, with its unique steric and electronic properties, affects the nanoparticle surface differently.

dx.doi.org/10.1021/cs200575r | ACS Catal. 2012, 2, 201−207

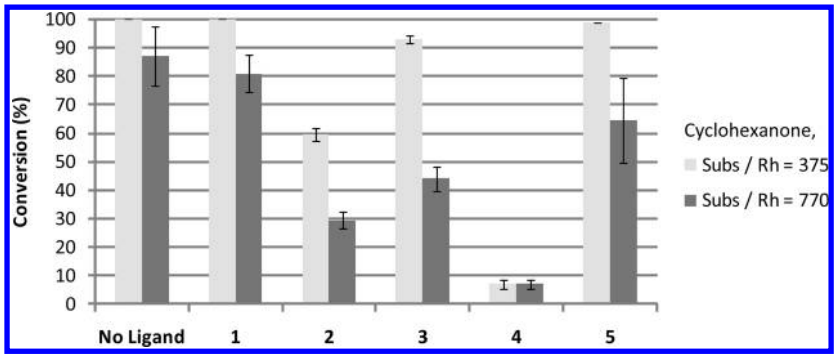

Figure 3. Hydrogenation of cyclohexanone by PVP-stabilized Rh nanoparticles in the presence of phosphine ligands **1**−**5**. PVP/Rh = 20, phosphine/Rh = 0.5. The only observed product was cyclohexanol. Conversions were determined by GC and are averages of two to four independent runs.

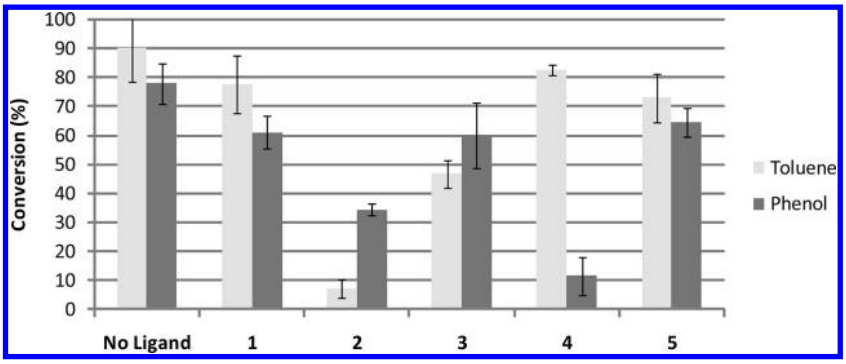

Figure 4. Hydrogenation of toluene and phenol by PVP-stabilized Rh nanoparticles in the presence of phosphine ligands **1**−**5**. PVP/Rh = 20, phosphine/Rh = 0.5, substrate/Rh = 375. For toluene, the only observed product was methylcyclohexane. For phenol, roughly equal amounts of cyclohexanone and cyclohexanol were observed. Conversions were determined by GC and are averages of two to four independent runs.

Scheme 2. Chemoselective Hydrogenation of Phenylacetone by PVP-Stabilized Rh Nanoparticles in the Presence of Phosphine Ligands

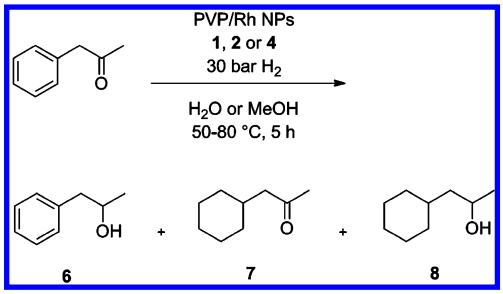

The IR spectrum of the phosphine-free control showed three $\nu(CO)_{ads}$ peaks, which is consistent with related systems.[13,20] The observed wavenumbers are close to those reported for linearly adsorbed CO on Rh colloids.[32] In the case of phosphines **1**, **3**, **4**, and **5**, the peak at highest wavenumber disappears and the peak at lowest wavenumber moves to an even lower position, which is as expected because the more basic phosphines should increase the electron density at the nanoparticle surface, leading to lower values for $\nu(CO)_{ads}$, increased back-bonding. Furthermore, $\nu(CO)_{ads}$ also depends on the CO coverage,[32] which in the present case may be related to phosphine sterics, and it would appear that the phosphines coordinate at specific sites, preferentially blocking CO

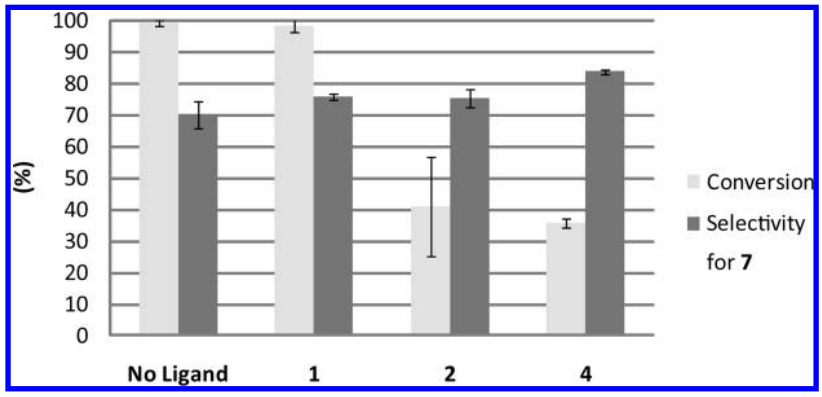

Figure 5. Chemoselective hydrogenation of phenylacetone by PVP-stabilized Rh nanoparticles in the presence of phosphine ligands **1**, **2**, or **4**. Reaction conditions: PVP/Rh = 20, phosphine/Rh = 0.5, substrate/Rh = 110, solvent = H_2O, T = 80 °C, p = 30 bar H_2, t = 5 h. Conversions were determined by GC and are averages of two independent runs.

dx.doi.org/10.1021/cs200575r | *ACS Catal.* 2012, 2, 201−207

Table 2. Optimization of Reaction Conditions for the Chemoselective Hydrogenation of Phenylacetone by PVP-Stabilized Rh Nanoparticles in the Presence of 4[a]

						selectivity		
entry	PVP/Rh	solvent	P/Rh	temp (°C)	conversion (%)	for **6** (%)	for **7** (%)	for **8** (%)
1	20	H_2O	0.0 (no ligand)	80	99	5	70	19
2	20	H_2O	0.5	80	36	9	84	2
3	10	H_2O	0.5	80	38	2	89	0
4	20	H_2O	0.1	80	81	6	90	5
5	10	H_2O	0.1	80	80	4	90	6
6	20	H_2O	0.1	50	66	6	92	2
7	20	H_2O	0.05	50	96	3	86	10
8	20	MeOH	0.1	50	100	0	84	4

[a]Conversions and selectivities are averages of two independent runs and were determined by GC. Pressure = 30 bar H_2, reaction time = 5 h. In some cases, small amounts of fully hydrogenated products, including propylcyclohexane, were detected in addition to **6**–**8**.

adsorption at those sites. It is noteworthy that the small and strongly basic phosphine, **2**, exhibits behavior different from the others, in which the intensity of two of the CO bands is significantly increased, which is possibly related to increased CO coverage at specific sites on the nanoparticle. It should be noted that the coordination properties of CO are different from the substrate molecules used herein, that is, toluene and cyclohexanone, and although the IR spectroscopic studies cannot be used to directly interpret the catalytic data, they show the dramatic influence that the phosphine ligands exert by blocking specific sites on the surface of the PVP-stabilized Rh nanoparticles.

The phosphines also affect the catalytic activity of the PVP-stabilized Rh nanoparticles to different extents, presumably by preventing binding of the substrate molecules to certain sites on the nanoparticle surface. It may be envisaged that smaller phosphines block a higher percentage of the available coordination sites than larger phosphines due to their reduced steric demand. The smallest phosphines are expected to generally be the most effective inhibitors, which is in keeping with our observations that show the two smallest phosphines, **2** and **3**, inhibit catalysis most effectively.

The electronic properties of the phosphines are expected to play a role, as well, although no clear correlation can be made between the electronic parameters of the ligands and the catalytic data. In addition, hydrophobic effects may play a role, and **4**, which contains hydrophobic groups, may help to repel the relatively hydrophilic phenol and cyclohexanone substrates, thereby preventing access of the substrate molecules to the nanoparticle surface. Thus, it may be argued that the hydrophobic phosphine, **4**, prevents hydrogenation of phenol and cyclohexanone, but not of toluene. A similar explanation has been used to explain the increased activity of Rh nanoparticles stabilized by hydrophobic derivatives of PVP in toluene hydrogenation.[13]

The PVP-Rh nanoparticles in the absence of a phosphine ligand afford **7** with a relatively high selectivity following the hydrogenation of the aromatic ring in phenylacetone. Similar effects have been observed previously in the hydrogenation of substituted aromatic compounds by carbon nanofiber-supported Pd- or Rh-nanoparticle-based catalysts in water.[6] The observed selectivity is probably due to the solvation of the polar ketone functionality in water, rendering its coordination to the nanoparticle surface less favorable. It should also be noted that following hydrogenation of the aromatic ring, the polarity of the compound decreases, reducing its solubility in water and, consequently, reducing the likelihood of further hydrogenation. Notably, the chemoselectivity of the reaction was found to increase significantly upon addition of phosphine ligand **4** (Figure 5 and Table 2). In this case, the selectivity toward arene hydrogenation, yielding product **7**, increased from 70% in the absence of phosphine ligand up to 92% in the presence of **4** under optimized conditions. This increase in chemoselectivity may be attributed to site blocking effects (see above) and also to the hydrophobicity of **4**, which may hinder the approach of the polar ketone functionality to the nanoparticle surface.

Finally, it has previously been shown that NPs can fragment into subnanometer (M_n) clusters, which may be the catalytically active species.[33] Specifically, it has been shown that Rh NPs can leach Rh_4 clusters that appear to catalyze benzene hydrogenation.[34] Consequently, we analyzed four samples by MALDI-TOF mass spectrometry, including Rh NPs (without a P ligand, before catalysis), Rh NPs (without a P ligand, after catalysis), ligand **1**-modified Rh NPs (after catalysis), and ligand **4**-modified Rh NPs (after catalysis), to see if any fragmentation could be observed. For all the samples, Rh_4 clusters were not detected (the MS spectra are provided in the Supporting Information), although a peak for Rh_1 is observed, but no peaks can be assigned to Rh-ligand species. From these data, it is not possible to conclude that molecular Rh species are the active catalysts, but one cannot exclude the possibility that the Rh NPs are actually precatalysts and not the active catalytic species.

4. CONCLUSIONS

The approach described herein of using ligands as NP catalyst modifiers has been transposed from heterogeneous catalysis, for which such strategies are not uncommon, to solvent dispersed systems. We showed that phosphine ligands with different steric and electronic properties and with differing polarities modify the properties of the nanoparticle surface and consequently influence their catalytic activity. The application of this strategy allowed the chemoselective hydrogenation of phenylacetone to cyclohexylacetone, via selective reduction of the aromatic ring, to be increased from 70 to 92%. The use of a completely water-soluble system with a well-defined Rh-to-phosphine ratio was essential for achieving this optimal chemoselectivity. Overall, this study shows the potential of ligands to be employed as selective poisons in nanocatalysis.

5. EXPERIMENTAL SECTION

5.1. General. Phosphines **1**–**5** were synthesized according to literature procedures.[35] All other chemicals were purchased from

dx.doi.org/10.1021/cs200575r | ACS Catal. 2012, 2, 201–207

commercial sources and used as received. Preparation of catalytic solutions was carried out in degassed solvents under a nitrogen atmosphere using Schlenk techniques. ^{31}P NMR spectra were recorded in CD_3OD or D_2O on a Bruker Avance II 400 spectrometer at 25 °C. GC analysis was performed on a Varian Chrompack CP-3380 using nitrogen as the carrier gas. Identification of compounds **6** and **7** by GC was achieved by comparison with commercially obtained authentic samples. Compound **8** was isolated and identified by ^{1}H and ^{13}C NMR spectroscopy.

5.2. Synthesis of Phosphine Selenides 1(Se)−5(Se). Phosphine selenides were obtained by stirring a solution of the phosphine (30−40 mg) in MeOH (2 mL) in the presence of 10 equiv of elemental selenium at 50 °C for 2 h. The mixtures were filtered over Celite and dried in vacuo, yielding white powders that were dissolved in the appropriate solvents and analyzed by NMR.

5.3. Preparation of Rh NP Solutions. $RhCl_3{\cdot}nH_2O$ (assay 42.64%, 0.121 g, 0.5 mmol) and PVP K-30 (0.55−1.1 g, 5.0−10 mmol) were added to a mixture of distilled H_2O (100 mL) and EtOH (100 mL). The solution was heated at reflux for 2 h, affording a black solution. The solvent was removed under vacuum, and distilled water was added (250 mL) to afford the PVP/Rh nanoparticle solution (C_{Rh} = 2.0 mM).

5.4. Catalytic Studies. Hydrogenation reactions were conducted in a multicell autoclave containing an internal temperature probe. Glass reactor vessels were charged with a solution of Rh NPs in water, a solution of phosphine ligand in water and a volume of substrate. The final concentration of Rh was 1.0 mM; that of phosphine ligand, 0.05−0.5 mM; and the final volume, 2.0 mL. The autoclave was sealed and purged with H_2 (3 × 10 bar), pressurized to 10−30 bar, and then either heated to 50−80 °C or stirred at RT. After reaction, the heating was stopped, and the autoclave was cooled to RT using an external water-cooling system, and the pressure was then released. Products were extracted with diethyl ether or *n*-hexane (5 mL) and analyzed by GC.

5.5. TEM. One drop of the Rh NP aqueous solution was placed on a copper grid coated with a carbon film. The grids were dried in air for 24 h at RT. TEM and HRTEM were performed on a JEOL JEM-2010 microscope operating at 300 keV.

5.6. IR Spectroscopy. PVP/Rh solutions in MeOH at a concentration of 20 mM Rh (i.e., 10× concentrated with respect to catalytic conditions) were mixed with 0.5 equiv of phosphines **1**−**5** at RT for 30 min in a glass vessel. The solutions were then placed under a CO atmosphere using a balloon and stirred at RT for 2 h. Several drops of the resulting solution were placed on a CaF_2 plate, and the solvent was allowed to evaporate to produce a film. The plate was then used for IR measurement on a PerkinElmer Spectrum GX FT-IR spectrophotometer with a resolution of 2.0 cm^{-1} using 128 accumulations per spectrum. Note that the amounts of Rh NPs measured for each sample were not identical, and therefore, the band intensity differences among different samples could not be used for direct comparison.

5.7. MALDI-TOF Mass Spectrometry. MALDI-TOF mass spectra were recorded on a Kratos Axima, CFR MALDI-TOF MS (Shimadzu Biotech, Kyoto Japan), using Kompact Software v.2.4.1. The mass spectrometer was set in linear mode for both positive and negative ion analysis. The dried droplet method was applied for all sample preparations. Briefly, the aqueous solution of the samples (1 mM Rh) was deposited (0.5 μL) onto the MALDI plate and dried at ambient temperature of 20 min before analysis. For P-ligand-modified Rh NPs, the P/Rh ratio was 0.1:1. No additional matrix was applied.

■ ASSOCIATED CONTENT

Supporting Information

TEM and HRTEM images and size distributions for samples containing ligands **1** and **2**, and IR spectra of samples after exposure to CO. This information is available free of charge via the Internet at http://pubs.acs.org/.

■ AUTHOR INFORMATION

Corresponding Author

*E-mail: paul.dyson@epfl.ch.

■ ACKNOWLEDGMENTS

The authors thank the EPFL and the Swiss National Science Foundation for funding. N. Yan thanks the EU for a Marie Curie International Incoming Fellowship within the seventh European Community Framework Program (No. 252125-TCPBRCBDP). Mr. Siyu Yao is acknowledged for carrying out the HRTEM analysis.

■ REFERENCES

(1) Widegren, J. A.; Finke, R. G. *J. Mol. Cat. A: Chem.* **2003**, *191*, 187.
(2) Roucoux, A. *Top. Organomet. Chem.* **2005**, *16*, 261.
(3) Gual, A.; Godard, C.; Castillon, S.; Claver, C. *Dalton Trans.* **2010**, *39*, 11499.
(4) Yan, N.; Xiao, C.; Kou, Y. *Coord. Chem. Rev.* **2010**, *254*, 1179.
(5) Kogan, V.; Aizenshtat, Z.; Neumann, R. *New J. Chem.* **2002**, *26*, 272.
(6) Anderson, J. A.; Athawale, A.; Imrie, F. E.; Mkenna, F. M.; Mcue, A.; Molyneux, D.; Power, K.; Shand, M.; Wells, R. P. K *J. Catal.* **2010**, *270*, 9.
(7) Bonilla, R. J.; James, B. R.; Jessop, P. G. *Chem. Commun.* **2000**, 941.
(8) Cimpeanu, V.; Kočevar, M.; Parvulescu, V. I.; Leitner, W. *Angew. Chem., Int. Ed.* **2009**, *48*, 1085.
(9) Januszkiewicz, K. R.; Alper, H. *Organometallics* **1983**, *2*, 1055.
(10) Julis, J.; Holscher, M.; Leitner, W. *Green Chem.* **2010**, *12*, 1634.
(11) Borsla, A.; Wilhelm, A. M.; Delmas, H. *Catal. Today* **2001**, *66*, 389.
(12) Pellegatta, J.-L.; Blandy, C.; Collière, V.; Choukroun, R.; Chaudret, B.; Cheng, P.; Philippot, K. *J. Mol. Catal. A: Chem.* **2002**, *178*, 55.
(13) Yan, N.; Zhang, J.-g.; Tong, Y.; Yao, S.; Xiao, C.; Li, Z.; Kou, Y. *Chem. Commun.* **2009**, 4423.
(14) Yan, N.; Yuan, Y.; Dyson, P. J. *Chem. Commun.* **2011**, *47*, 2529.
(15) Astruc, D.; Lu, F.; Aranzaes, J. R. *Angew. Chem., Int. Ed.* **2005**, *44*, 7852.
(16) Roucoux, A.; Philippot, K. In *Handbook of Homogeneous Hydrogenation*, 1st ed.; De Vries, J. G., Elsevier, C. J., Eds.; Wiley-VCH: Weinheim, 2007; Vol. *1*.
(17) Pachón, L. D.; Rothenberg, G. *Appl. Organomet. Chem.* **2008**, *22*, 288.
(18) Ashida, T.; Miura, K.; Nomoto, T.; Yagi, S.; Sumida, H.; Kutluk, G.; Soda, K.; Namatame, H.; Taniguchi, M. *Surf. Sci.* **2007**, *601*, 3898.
(19) Chaudret, B. *Top. Organomet. Chem.* **2005**, *16*, 233.
(20) Dykeman, R. R.; Yan, N.; Scopelliti, R.; Dyson, P. J. *Inorg. Chem.* **2011**, *50*, 717.
(21) Smith, G. V.; Notheisz, F. *Heterogeneous Catalysis in Organic Chemistry*; Academic Press: San Diego, 1999.
(22) Blaser, H.-U.; Malan, C.; Pugin, B.; Spindler, F.; Steiner, H.; Studer, M. *Adv. Synth. Catal.* **2003**, *345*, 103.
(23) Mori, A.; Miyakawa, Y.; Ohashi, E.; Haga, T.; Maegawa, T.; Sajiki, H. *Org. Lett.* **2006**, *8*, 3279.
(24) Hornstein, B. J.; Aiken, J. D.; Finke, R. G. *Inorg. Chem.* **2002**, *41*, 1625.
(25) Notheisz, F.; Zsigmond, A.; Bartok, M.; Szegletes, Z.; Smith, G. V. *Appl. Catal., A* **1994**, *120*, 105.
(26) Gonzalez-Tejuca, L.; Aika, K.; Namba, S.; Turkevich, J. *J. Phys. Chem.* **1977**, *81*, 1399.
(27) Moiseev, I. I.; Vargaftik, M. N. *New J. Chem.* **1998**, *22*, 1217.
(28) Schmid, G.; Emde, S.; Maihack, V.; Meyer-Zaika, W.; Peschel, S. *J. Mol. Catal A: Chem.* **1996**, *107*, 95.
(29) Allen, D. W.; Taylor, B. F. *J. Chem. Soc., Dalton Trans.* **1982**, 51.
(30) Allen, D. W.; Nowell, I. W.; Taylor, B. F. *J. Chem. Soc., Dalton Trans.* **1985**, 2505.

(31) Genin, E.; Amengual, R.; Michelet, V.; Savignac, M.; Jutand, A.; Neuville, L.; Genêt, J.-P. *Adv. Synth. Catal.* **2004**, *346*, 1733.
(32) Mucalo, M. R.; Cooney, R. P. *Chem. Mater.* **1991**, *3*, 1081.
(33) Widegren, J. A.; Finke, R. G. *J. Mol. Catal. A: Chem* **2003**, *198*, 317.
(34) Bayram, E.; Linehan, J. C.; Fulton, J. L.; Roberts, J. A. S.; Szymczak, N. K.; Smurthwaite, T. D.; Ozkar, S.; Balasubramanian, M.; Finke, R. G. *J. Am. Chem. Soc.* **2011**, *133*, 18889.
(35) Gan, W.; Fellay, C.; Dyson, P. J.; Laurenczy, G. *J. Coord. Chem.* **2010**, *63*, 2685.